EVALUATION OF THE EFFECTIVENESS OF STRENGTHENING THE FOUNDATION SOIL OF MULTI-STOREY BUILDINGS USING A SOIL CUSHION AND DEEP SOIL MIXING TECHNOLOGY IN REDUCING SEISMIC EFFECTS

Sh.S. Yuldashev[1], M.B. Boytemirov[2], A.Sh. Abdunazarov[3]
Doctor of Technical Sciences, Professor, Namangan State Technical University[1]
PhD in Technical Sciences, Docent, Namangan State Technical University[2]
PhD Student, Namangan State Technical University[3]
https://doi.org/10.5281/zenodo.20697242

Abstract. *This article analyzes the effectiveness of a soil cushion and Deep Soil Mixing technology in reducing the impact of seismic waves, taking into account the physical and mechanical properties of the foundation and foundation soil of a multi-storey building. A 12-storey building and the underlying soil mass were selected as the research object, and the calculations were performed in PLAXIS 3D using the finite element method. In the numerical model, the geometric and physical-mechanical properties of the building, foundation, natural soil, soil cushion, and Deep Soil Mixing elements were considered. The seismic action was applied based on a real accelerogram, and observation points were assigned at the basement level, on each floor, and at the roof level of the building. Three cases were compared in the study: the natural soil condition, the case with a soil cushion, and the case with Deep Soil Mixing technology. The results showed that, under natural soil conditions, displacement, velocity, and acceleration values increased as the building height increased. When a soil cushion was applied, the reduction efficiency was 2.63–8.84% for displacement, 4.40–16.02% for velocity, and 4.69–15.68% for acceleration. When Deep Soil Mixing was applied, displacement decreased by 9.41–22.61%, velocity by 3.65–17.91%, and acceleration by 6.18–20.97%. The soil cushion reduced the dynamic response of the building to a certain extent; however, Deep Soil Mixing technology demonstrated relatively higher efficiency in reducing displacement and acceleration. Therefore, for multi-storey buildings located in seismically active regions, strengthening the foundation soil using Deep Soil Mixing can be considered an appropriate engineering solution.*

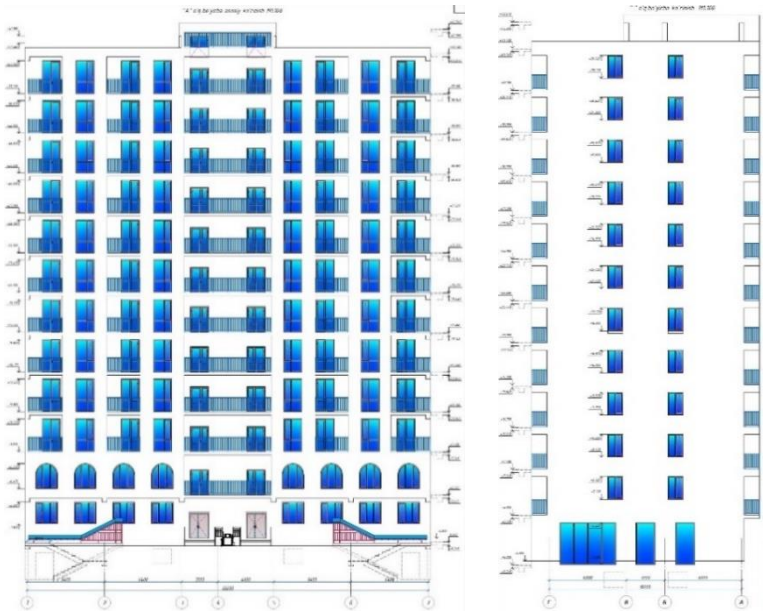
Keywords: *soil cushion, Deep Soil Mixing, settlement, foundation, weak soil, differential settlement, numerical modelling, PLAXIS 3D.*

INTRODUCTION

In modern construction practice, when multi-storey buildings are constructed on weak and highly compressible soils, the occurrence of total and differential settlements is inevitable. This leads to the development of additional stresses in structural elements, uneven distribution of deformations, and, in some cases, a decrease in the operational reliability of the structure. In particular, for 10–15-storey buildings, both the magnitude of settlement and its non-uniformity represent an important engineering problem [1].

Numerous scientific studies have been conducted to investigate the behaviour mechanism of foundations on weak soils and to develop methods for reducing settlement. In classical studies,

soil compressibility, deformation modulus, and consolidation processes under loading have been considered as the main factors. In particular, the consolidation theory developed by Chen Fang and his colleagues forms a fundamental basis for calculating soil settlement. In later studies, factors such as the nonlinear properties of soil, loading rate, and interlayer interaction were also taken into account [2].



a. ***b.***

Figure 1. Front and side views of the building

In recent years, modern methods of foundation soil improvement have been widely developed, among which soil cushions and Deep Soil Mixing technology occupy a special place [3]. Woods (1968) studied the issues of reducing wave propagation in soil masses and redistributing loads. These studies demonstrated that deformations can be reduced by artificially improving the soil, and the effectiveness of column-type reinforcement systems was substantiated by the researcher [4].

A soil cushion reduces contact pressures by distributing the load over a wider area in the upper layer and makes deformations relatively more uniform. However, the effect of this method is mainly limited to near-surface layers [5]. In contrast, Deep Soil Mixing technology provides high strength and deformation resistance in deeper layers by cementing the soil. Deep Soil Mixing columns transfer loads to deeper layers, reduce total settlement, and increase the overall stiffness of the foundation soil [6].

Although a number of modern studies have demonstrated the effectiveness of using soil cushions and column-type reinforcement methods separately [7], the issue of their combined application has not been studied in sufficient depth. This problem remains especially relevant for multi-storey buildings, where deformation control in both upper and deeper soil layers is required simultaneously.

MATERIALS AND METHOD

The problem of studying the effect of seismic waves on a building is considered as a three-dimensional dynamic problem of the theory of elasticity in an infinite medium. Since the solution domain has a complex geometry and is heterogeneous, obtaining an analytical solution is not feasible. Therefore, the finite element method, which is convenient for solving such problems, was used. As is known, the finite element method can only be applied to a finite domain. For this

reason, a finite region of interest is conceptually extracted from the infinite medium, and non-reflecting boundary conditions are applied at its boundaries to allow waves to pass through without reflection.

In solving this problem, the selected computational model was assumed to be a soil mass with a length of 300 m, a width of 50 m, and a depth of 30 m. The groundwater level was located at a depth of 1.5 m. The building has a rectangular plan with a length of 33.2 m and a width of 15 m. The basement depth is 2.7 m, the plinth height is 0.6 m, the storey height is 3.3 m, and the total height of the building is 40.2 m (Figure 1).

To ensure that seismic waves propagate from the boundaries of the computational domain into the infinite medium without reflection, special boundary conditions were applied on the ADHJ, BCEF, ADCB, HJFE, and AHBE faces of the parallelepiped. The scheme for applying the boundary conditions is shown in Figure 2.

$$\text{ADHJ da } \left.\begin{aligned}\sigma_x &= a\rho V_p \dot{u}\\ \tau_{xy} &= b\rho V_s \dot{v}\\ \tau_{xz} &= b\rho V_s \dot{w}\end{aligned}\right\},\qquad \text{BCEF da } \left.\begin{aligned}\sigma_x &= -a\rho V_p \dot{u}\\ \tau_{xy} &= -b\rho V_s \dot{v}\\ \tau_{xz} &= -b\rho V_s \dot{w}\end{aligned}\right\},$$

$$\text{ADCB da } \left.\begin{aligned}\sigma_y &= a\rho V_p \dot{u}\\ \tau_{yz} &= b\rho V_s \dot{w}\\ \tau_{yx} &= b\rho V_s \dot{v}\end{aligned}\right\},\qquad \text{HJFE da } \left.\begin{aligned}\sigma_y &= -a\rho V_p \dot{u}\\ \tau_{yz} &= -b\rho V_s \dot{w}\\ \tau_{yx} &= -b\rho V_s \dot{v}\end{aligned}\right\},$$

$$\text{AHBE da } \left.\begin{aligned}\sigma_z &= a\rho V_p \dot{w}\\ \tau_{zy} &= b\rho V_s \dot{u}\\ \tau_{zx} &= b\rho V_s \dot{v}\end{aligned}\right\} \qquad (1)$$

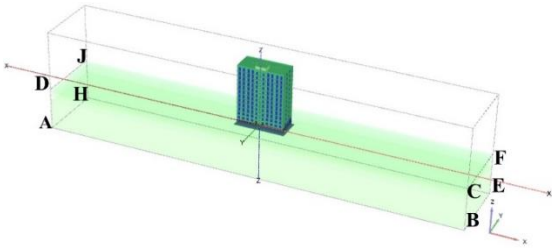


Figure 2. Application of boundary conditions

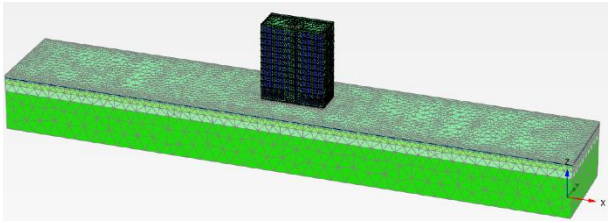


Figure 3. Finite element discretization of the model

The study domain was discretized into 47,473 finite elements and 99,354 nodes. The finite elements had the form of irregular tetrahedra. The order of the system of differential equations of motion was 298,062 (Figure 3).

The kinematic relation can be formulated as follows [8]:

$$\varepsilon = Lu \qquad (2)$$

L^T - transposed differential operator

$$L^T = \begin{bmatrix} \frac{\partial}{\partial x} & 0 & 0 & \frac{\partial}{\partial y} & 0 & \frac{\partial}{\partial z} \\ 0 & \frac{\partial}{\partial y} & 0 & \frac{\partial}{\partial x} & \frac{\partial}{\partial z} & 0 \\ 0 & 0 & \frac{\partial}{\partial z} & 0 & \frac{\partial}{\partial y} & \frac{\partial}{\partial x} \end{bmatrix} \qquad (3)$$

In the particular case of a plane stress state, the three strain components corresponding to the stress state are written as follows [9]:

$$\{\sigma\} = \begin{Bmatrix} \sigma_{xx} & \tau_{xy} & \tau_{xz} \\ \tau_{xy} & \sigma_{yy} & \tau_{yz} \\ \tau_{xz} & \tau_{yz} & \sigma_{zz} \end{Bmatrix} \quad (4)$$

The matrix ([D]) is determined from the following relationship between stress and strain [10]:

$$\begin{aligned} \varepsilon_x - (\varepsilon_x)_0 &= \frac{1}{E}\sigma_x - \frac{v}{E}(\sigma_y + \sigma_z); \\ \varepsilon_y - (\varepsilon_y)_0 &= \frac{1}{E}\sigma_y - \frac{v}{E}(\sigma_x + \sigma_z); \\ \varepsilon_z - (\varepsilon_z)_0 &= \frac{1}{E}\sigma_z - \frac{v}{E}(\sigma_x + \sigma_y); \\ \gamma_{ij} - (\gamma_{ij})_0 &= \frac{2(1+v)}{E}\tau_{ij}; \end{aligned} \quad (5)$$

From this:

$$[D] = \frac{E}{1-v^2}\begin{bmatrix} 1 & v & 0 \\ v & 1 & 0 \\ 0 & 0 & \frac{1-v}{2} \end{bmatrix} \quad (6)$$

The system of second-order linear differential equations describing the time-dependent motion of the volume under the action of dynamic loading is expressed as follows [8,11]:

$$[\boldsymbol{M}]\{\ddot{\boldsymbol{u}}(\boldsymbol{t})\} + [\boldsymbol{C}]\{\dot{\boldsymbol{u}}(\boldsymbol{t})\} + [\boldsymbol{K}]\{\boldsymbol{u}(\boldsymbol{t})\} = \{\boldsymbol{F}(\boldsymbol{t})\} \quad (7)$$

where $[\boldsymbol{M}]$ is the mass matrix, $[\boldsymbol{C}]$ is the damping matrix, $[\boldsymbol{K}]$ is the stiffness matrix, and $\{\boldsymbol{F}(\boldsymbol{t})\}$ is the dynamic load vector. The vectors $\{\boldsymbol{u}(\boldsymbol{t})\}$, $\{\dot{\boldsymbol{u}}(\boldsymbol{t})\}$ and $\{\ddot{\boldsymbol{u}}(\boldsymbol{t})\}$ representing displacement, velocity, and acceleration, respectively, were assumed to be continuous functions of time.

The obtained system was formulated based on the finite element method and solved numerically using the PLAXIS 3D software package. The general properties of the building, soil, soil cushion, and Deep Soil Mixing elements are presented in Table 1.

Table 1

Name	Unit	Symbol	Layers				
			Layer 1	Layer 2	Layer 3	Layer 4	Layer 5
General properties of the soil							
Soil model	Mohr–Coulomb						
Layer thickness	m	m	0,80	1,70	2,50	4,00	21,00
Unsaturated unit weight of soil	kN/m^3	γ_{unsat}	17	18	18	19	20
Saturated unit weight of soil	kN/m^3	γ_{sat}	18	19	19	20	21
Young's modulus	kN/m^2	E	10 000	40 000	60 000	45 000	60 000
Poisson's ratio	–	v	0,38	0,30	0,30	0,30	0,30
Internal friction angle	º	φ	19,2	31	18	33	35

Effective cohesion of soil	kN/m^2	c'_{ref}	10	1	24	45	0

General properties of the building			
Name	Unit	Symbol	Value
Model type	Elastic		
Young's modulus	kN/m^2	E	27 000 000
Poisson's ratio	–	v	0.2
Unit weight	kN/m^3	γ	24
Properties of the soil cushion			
Soil model	Mohr–Coulomb		
Unsaturated unit weight of soil	kN/m^3	γ_{unsat}	18,5
Saturated unit weight of soil	kN/m^3	γ_{sat}	19,5
Young's modulus	kN/m^2	E	95 000
Poisson's ratio	–	v	0,3
Internal friction angle	°	φ	36
Dilation angle	°	ψ	3
Depth	m	–	4
Properties of Deep Soil Mixing elements			
Model type	–	–	Elastic
Young's modulus	kN/m^2	E	8 000 000
Poisson's ratio	–	v	0.2
Unit weight	kN/m^3	γ	20
Cross-sectional area	m^2	A	0,283
Moment of inertia about the z-axis	m^4	I_2	$6{,}36 \cdot 10^{-3}$
Moment of inertia about the y-axis	m^4	I_3	$6{,}36 \cdot 10^{-3}$
Diameter	m	–	0,6
Depth	m	–	12
Number of elements	pcs	–	231

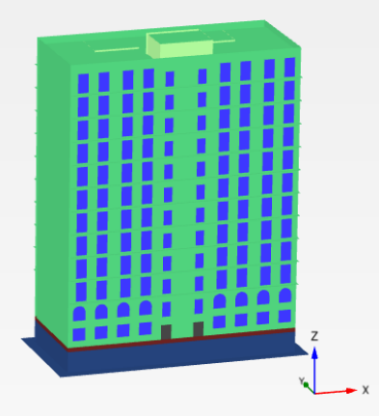


Figure 4. Building under natural ground conditions

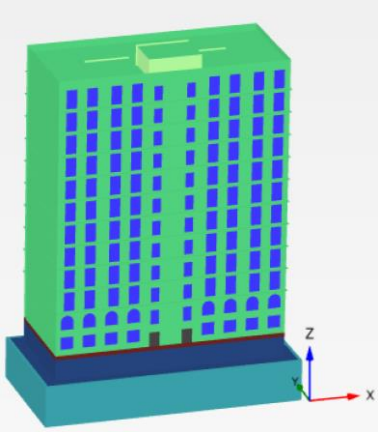


Figure 5. Building with a soil cushion

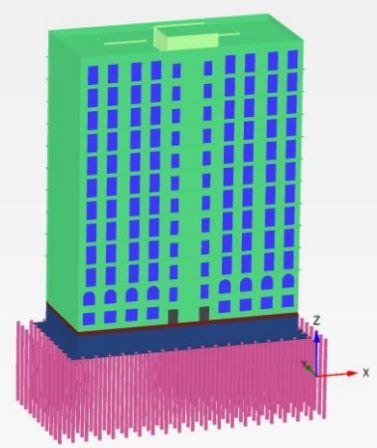


Figure 6. Building with Deep Soil Mixing

Based on the parameters presented in Table 1, a three-dimensional computational model of the building was developed. The model was formed taking into account the architectural

planning and structural design solutions of the building. The main geometric dimensions of the building, the floor configuration, and the load-bearing structural elements were considered in the numerical model. Based on this model, three computational cases were analyzed. In the first case, the building was modeled under natural ground conditions (Figure 4). In the second case, a 4 m thick soil cushion was placed beneath the building foundation (Figure 5). In the third case, Deep Soil Mixing elements were modeled beneath the building foundation, with a diameter of 0.6 m, a length of 12 m, a spacing of 2 m, and a total number of 231 elements (Figure 6).

In order to determine and compare the seismic waves affecting the building, one observation point was assigned on each floor of the building, making a total of 12 points, and additional observation points were also selected at the basement level and at the roof level of the building (Figure 7).

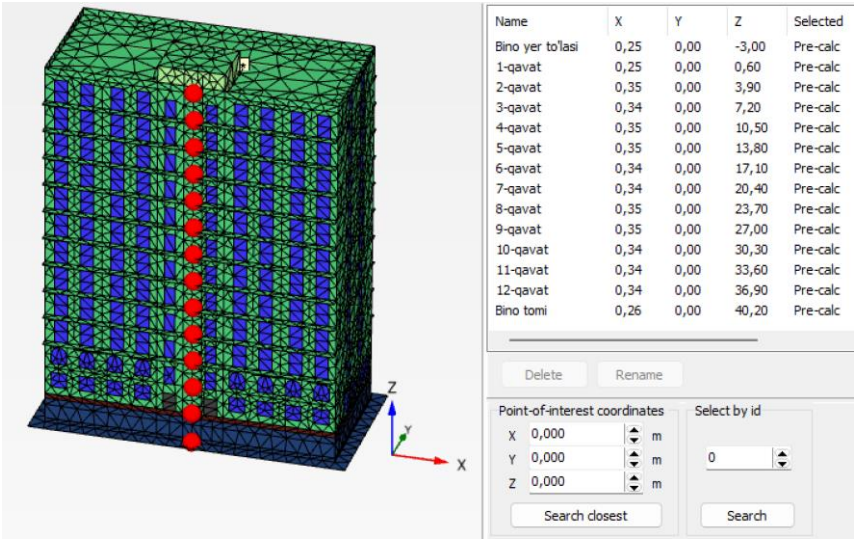


Figure 7. Observation points in the building

Seismic wave propagation was generated using a real accelerogram (Figure 8).

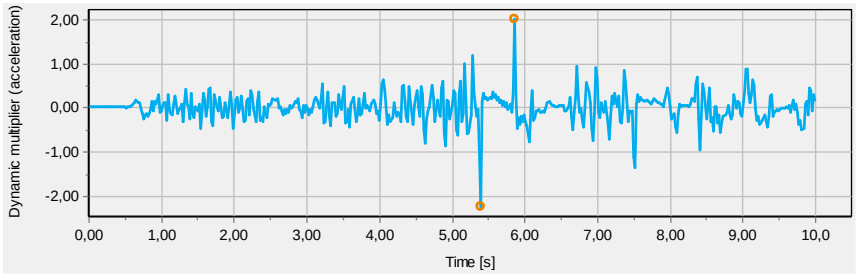


Figure 8. Real accelerogram [12] (The accelerogram coordinates were x=37.95 and y=67.02, with a magnitude of M=5.8).

In dynamic analyses, the proper selection of boundary conditions plays an important role in reducing the artificial reflection of seismic waves from the model boundaries. Therefore, in the PLAXIS 3D model, **Free-field** boundary conditions were assigned to the lateral boundaries X_{min} and X_{max}. For the bottom boundary Z_{min}, a **Compliant base** condition was adopted, since the seismic motion was applied to the model through this boundary. No special dynamic boundary condition was applied at the Y_{min} and Y_{max} boundaries or at the upper boundary Z_{max}. The Z_{max} boundary was considered as a free surface representing the ground surface.

RESULTS AND DISCUSSION

During the numerical modelling process, the seismic excitation applied on the basis of a real accelerogram propagated through the soil mass and was transmitted to the structure through the building foundation. The process of seismic wave propagation in the soil is presented in Figure 9.

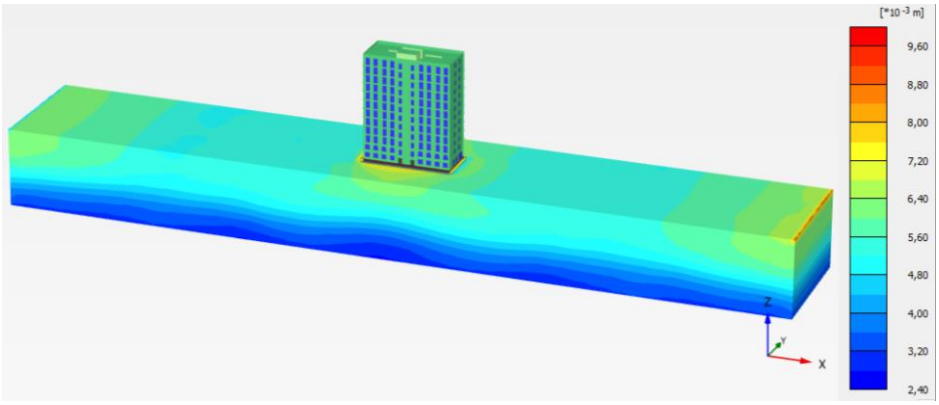


Figure 9. Process of seismic wave impact on the building

Based on the results of the numerical modelling, the maximum amplitude values of displacement, velocity, and acceleration in the building were determined, summarized in Table 2, and comparatively analyzed in terms of their effectiveness.

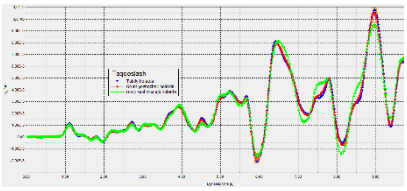


Figure 10. Time-history comparison graph of displacements at the basement level of the building

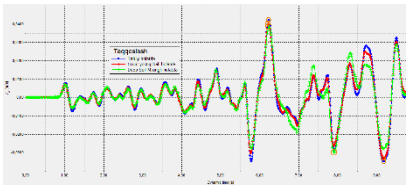


Figure 11. Time-history comparison graph of velocities at the basement level of the building

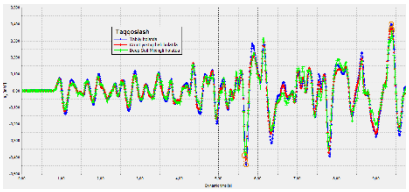


Figure 12. Time-history comparison graph of accelerations at the basement level of the building

The results obtained for the basement level of the building showed that strengthening the soil foundation leads to a reduction in dynamic parameters. Under natural soil conditions, the displacement at the basement level of the building was 10.77 mm. When a soil cushion was applied, the displacement decreased to 10.49 mm, corresponding to an efficiency of 2.63%. When Deep Soil Mixing technology was applied, the displacement decreased to 9.52 mm, and the efficiency reached 11.67% (Figure 10).

The velocity value under natural conditions was 4.21 cm/s, and when a soil cushion was applied, it decreased to 4.03 cm/s. In this case, the reduction efficiency in terms of velocity was 4.40%. When Deep Soil Mixing technology was applied, the velocity decreased to 3.84 cm/s, and the efficiency reached 8.77% (Figure 11).

The acceleration value under natural soil conditions was 0.446 m/s². When a soil cushion was applied, the acceleration decreased to 0.416 m/s², corresponding to an efficiency of 6.63%. When Deep Soil Mixing technology was applied, the acceleration decreased to 0.390 m/s², and the efficiency reached 12.36% (Figure 12). These results indicate that, at the basement level of the building, Deep Soil Mixing technology demonstrates higher effectiveness compared with the soil cushion.

The results obtained for the roof level of the building showed that strengthening the soil foundation also leads to a reduction in dynamic parameters at the upper floors. Under natural soil conditions, the displacement at the roof level of the building was 17.28 mm. When a soil cushion was applied, the displacement decreased to 16.54 mm, corresponding to an efficiency of 4.28%. When Deep Soil Mixing technology was applied, the displacement decreased to 15.55 mm, and the efficiency reached 10.02% (Figure 13).

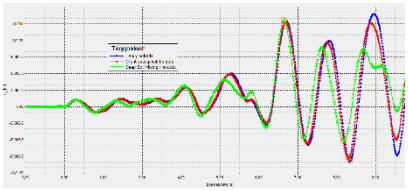


Figure 13. Time-history comparison graph of displacements at the roof level of the building

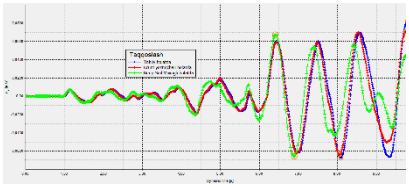


Figure 14. Time-history comparison graph of velocities at the roof level of the building

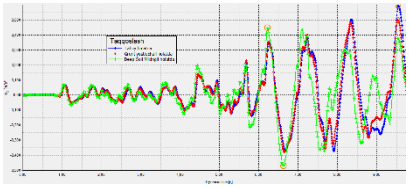


Figure 15. Time-history comparison graph of accelerations at the roof level of the building

The velocity value under natural conditions was 8.21 cm/s, and when a soil cushion was applied, it decreased to 7.09 cm/s. In this case, the reduction efficiency in terms of velocity was 13.56%. When Deep Soil Mixing technology was applied, the velocity decreased to 6.74 cm/s, and the efficiency reached 17.91% (Figure 14).

The acceleration value under natural soil conditions was 0.594 m/s². When a soil cushion was applied, the acceleration decreased to 0.501 m/s², corresponding to an efficiency of 15.68%. When Deep Soil Mixing technology was applied, the acceleration decreased to 0.469 m/s², and the efficiency reached 20.97% (Figure 15). These results indicate that, at the roof level of the building, Deep Soil Mixing technology demonstrates higher effectiveness in reducing seismic vibrations compared with the soil cushion.

Table 2

№	Observation points	Natural condition			Soil cushion						Deep Soil Mixing					
		Displacement, mm	Velocity, cm/s	Acceleration, m/s²	Displacement, m	Efficiency, %	Velocity, cm/s	Efficiency, %	Acceleration, m/s²	Efficiency, %	Displacement, mm	Efficiency, %	Velocity, cm/s	Efficiency, %	Acceleration, m/s²	Efficiency, %
1	Basement level of the building	10,77	4,21	0,446	10,49	2,63%	4,03	4,40%	0,416	6,63%	9,52	11,67%	3,84	8,77%	0,390	12,36%
2	1st floor	11,23	3,97	0,406	10,8	3,83%	3,78	4,70%	0,379	6,73%	9,33	16,84%	3,71	6,49%	0,364	10,33%
3	2nd floor	11,69	3,78	0,388	11,12	4,85%	3,58	5,20%	0,369	4,91%	9,17	21,57%	3,64	3,65%	0,347	10,71%
4	3rd floor	12,16	3,97	0,386	11,46	5,77%	3,63	8,56%	0,368	4,69%	9,41	22,61%	3,64	8,20%	0,328	15,12%
5	4th floor	12,64	4,18	0,381	11,81	6,59%	3,75	10,28%	0,363	4,83%	10,01	20,79%	3,72	10,99%	0,334	12,39%
6	5th floor	13,12	4,42	0,372	12,17	7,29%	3,88	12,20%	0,353	5,27%	10,64	18,94%	3,86	12,57%	0,333	10,60%
7	6th floor	13,6	4,67	0,361	12,53	7,90%	4,01	14,17%	0,340	5,95%	11,27	17,13%	4,06	13,19%	0,330	8,77%
8	7th floor	14,07	4,94	0,346	12,89	8,41%	4,14	16,02%	0,322	6,93%	11,9	15,42%	4,35	11,81%	0,322	6,93%
9	8th floor	14,54	5,20	0,337	13,25	8,84%	4,58	12,00%	0,314	6,93%	12,54	13,77%	4,74	8,89%	0,316	6,18%
10	9th floor	15	5,79	0,363	13,69	8,73%	5,07	12,35%	0,337	7,08%	13,16	12,24%	5,12	11,51%	0,330	9,08%
11	10th floor	15,44	6,40	0,410	14,42	6,65%	5,57	13,03%	0,366	10,57%	13,77	10,83%	5,50	14,18%	0,366	10,72%
12	11th floor	15,88	7,01	0,469	15,14	4,72%	6,09	13,23%	0,402	14,38%	14,37	9,52%	5,87	16,34%	0,401	14,53%
13	12th floor	16,52	7,61	0,531	15,84	4,09%	6,59	13,41%	0,451	15,22%	14,96	9,41%	6,30	17,25%	0,435	18,07%
14	Roof level of the building	17,28	8,21	0,594	16,54	4,28%	7,09	13,56%	0,501	15,68%	15,55	10,02%	6,74	17,91%	0,469	20,97%

CONCLUSION

In this study, the effectiveness of strengthening the foundation soil beneath a multi-storey building using a soil cushion and Deep Soil Mixing technology in reducing seismic effects was

evaluated through numerical modelling using the PLAXIS 3D software package. In the calculations, three cases were compared: the natural soil condition, the case with a soil cushion, and the case with Deep Soil Mixing technology. To assess the dynamic response of the building, displacement, velocity, and acceleration values were analyzed at the basement level, floor levels, and roof level.

The obtained results showed that, under natural soil conditions, the dynamic parameters increased with the height of the building. In particular, the displacement under natural conditions was 10.77 mm at the basement level and increased to 17.28 mm at the roof level. The velocity increased from 4.21 cm/s to 8.21 cm/s, while the acceleration increased from 0.446 m/s² to 0.594 m/s². This indicates that the vibration amplitudes increase at the upper floors as a result of seismic excitation.

When a soil cushion was applied, a reduction in dynamic parameters was observed at all observation points. In this case, the reduction efficiency ranged from 2.63% to 8.84% for displacement, from 4.40% to 16.02% for velocity, and from 4.69% to 15.68% for acceleration. The average efficiency was 6.04% for displacement, 10.94% for velocity, and 8.27% for acceleration. These results indicate that the soil cushion redistributes stresses and deformations beneath the building foundation to a certain extent.

When Deep Soil Mixing technology was applied, relatively higher efficiency was achieved. In this case, displacement values decreased by 9.41–22.61%, velocity values by 3.65–17.91%, and acceleration values by 6.18–20.97% compared with the natural soil condition. The average efficiency was 15.05% for displacement, 11.55% for velocity, and 11.91% for acceleration. In particular, the reduction of acceleration by up to 20.97% at the roof level demonstrates that DSM technology is effective in reducing seismic effects at the upper floors of the building.

The comparative results showed that although the soil cushion has a positive effect in reducing seismic vibrations, Deep Soil Mixing technology provides higher efficiency in reducing displacement and acceleration. This can be explained by the fact that DSM elements increase the overall stiffness of the soil mass, transfer loads to deeper layers, and improve the dynamic stability of the building–foundation–soil system.

For multi-storey buildings located in seismically active regions, strengthening weak foundation soils using Deep Soil Mixing technology can be considered an appropriate engineering solution. However, the obtained results are valid for the selected numerical model, soil parameters, building geometry, and applied accelerogram conditions. Therefore, further studies are recommended using different seismic records, soil types, and arrangement schemes of DSM elements.

REFERENCES

1. Nishi, R., Fujiwara, J., Kajiwara, K., Mizutani, K., & Nagae, T. (2026). Seismic response and damage of nonstructural components observed via a full-scale shake table test on a 10-story steel building. *Engineering Structures*, *354*, 122388. https://doi.org/10.1016/j.ijantimicag.2020.105949
2. Fang, C., Yosef, T. Y., Steelman, J. S., Faller, R. K., & Kim, S. (2025). Dynamic impact response and crashworthiness of luminaire pole-foundation systems in weak cohesionless soil. *Engineering Structures*, *343*, 121102. https://doi.org/10.1016/j.engstruct.2025.121153
3. Alavi, S. M., Aghamolaei, M., Talarposhti, S. S., & Ardabili, A. A. K. (2025). Requirements of efficient deep soil mixing treatment in clayey soils: a field-based assessment of water

predrilling and auger free blade effects. *Canadian Geotechnical Journal*, *62*, 1-20. https://doi.org/10.1520/GTJ20130099

4. Woods, R. D. (1968). Screening of surface wave in soils. Journal of the soil mechanics and foundations division, 94(4), 951-979. https://doi.org/10.1061/JSFEAQ.0001180
5. Dubreucq, T., & Thorel, L. (2025). Low thickness platform on soft soil reinforced with rigid inclusions: 2D rolling load tests in centrifuge. *Transportation Geotechnics*, 101800. https://doi.org/10.1016/j.trgeo.2025.101800
6. Uge, B. U., Guo, Y., Zhao, J., Liu, Y., Li, Y., Hou, S., ... & Xia, Y. (2025). Load-Transfer Analysis of Disconnected Piled Raft in unsaturated soils: Application and Validation of the modified shear displacement method. *Results in Engineering*, 107684. https://doi.org/10.1016/j.rineng.2025.107684
7. Aligholi, H. Z., & Bozbey, I. (2025). Laboratory investigation of strength evolution in organic soils improved by deep mixing method. *Transportation Geotechnics*, *52*, 101589. https://doi.org/10.1016/j.trgeo.2025.101589
8. Sharafitdin Yuldashev, Akbarjon Abdunazarov, Shirin Jumaboyeva, Muhammadbobir Boytemirov, Yodgor Tillaboyev; Attenuation of seismic surface waves affecting the building using various barriers. AIP Conf. Proc. 3 April 2025; 3265 (1): 030016. https://doi.org/10.1063/5.0265304
9. Il'ichev, V. A., Yuldashev, S. S., & Matkarimov, P. Z. (1999). Forced vibrations of an inhomogeneous planar system with passive vibrational insulation. *Soil Mechanics and Foundation Engineering*, *36*(2), 50-54. https://doi.org/10.1007/BF02469084
10. Il'ichev, V. A., Yuldashev, S. S., & Saidov, S. M. (1999). Propagation of vibration from trains in relation to track position. *Soil Mechanics and Foundation Engineering*, *36*(2), 55-56. https://doi.org/10.1007/BF02469085
11. Mirsaidov, M., Boytemirov, M., & Yuldashev, F. (2021). Estimation of the Vibration Waves Level at Different Distances. In Proceedings of FORM 2021: Construction The Formation of Living Environment (pp. 207-215). Cham: Springer International Publishing. https://doi.org/10.1007/978-3-030-79983-0_19
12. Ismailov V.A., Nurmatov U.A., Ibragimov A.X., Yodgorov SH.I., Yadigarov E.M., Aktamov B.U., Bozorov J.SH. O posledstviyax Baysunskogo-3 (Chilanzarskogo) zemletryaseniya 12.05.2022 yil/SEYSMOLOGIYA MUAMMOLARI TOSHKENT-2022/№1 S.3-12.